

Identifying the Energy of Low-velocity Impacts on Composite Components Using Acoustic Emission

Li Ai
University of South Carolina
300 Main St
Columbia, SC 29201
ail@email.sc.edu

Bryson Henderson
University of South Carolina
1000 Catawba St Suite 120
Columbia, SC 29201
BRYSONPH@email.sc.edu

Sydney Houck
University of South Carolina
1000 Catawba St Suite 120
Columbia, SC 29201
smhouck@email.sc.edu

Samuel. Dickson
University of South Carolina
1000 Catawba St Suite 120
Columbia, SC 29201
samuelwd@email.sc.edu

Paul Ziehl
University of South Carolina
301 Main St
Columbia, SC 29201
ziehl@cec.sc.edu

Abstract—Low-velocity impacts (LVI) caused by debris and hail can be one of the main threats to the integrity of aircraft components. Identifying the energy levels of LVI is critical to assessing the damage caused by the impacts on the aircraft. The traditional approach to identifying the energy of impacts is the C-Scan using the ultrasonic technique. However, this assessment cannot be used in real-time and is only available between flight missions. Moreover, the C-Scans are performed manually and can be affected by human errors. However, thanks to recent advances in sensing technology, structural health monitoring methods such as acoustic emission monitoring can now be applied to composite impact assessment. The innovation of this paper lies in the development of an impact energy assessment system using one acoustic emission sensor. In this system, a deep convolutional neural network was used to identify the impact energies and classify the impacts into five levels. The results demonstrate the effectiveness and potential of the proposed framework.

TABLE OF CONTENTS

1. INTRODUCTION.....	1
2. METHODOLOGY	2
3. EXPERIMENTAL DESCRIPTION.....	3
4. RESULTS AND DISCUSSION	3
5. CONCLUSIONS.....	5
ACKNOWLEDGEMENT	5
REFERENCES.....	5
BIOGRAPHY	6

1. INTRODUCTION

Low-velocity impacts (LVI) are one of the biggest threats to the structural integrity of composite aircraft components. Typically, traditional C-Scan examination is used to evaluate

impact damage. However, this method is time-consuming and prone to human mistakes, moreover, this assessment is not real-time and is only available between flight missions. Recent developments in sensor technology and data processing techniques have made it possible to employ structural health monitoring systems to automatically find impacts and evaluate the damage. This can be used in conjunction with manual scanning.

Acoustic emission (AE) is a structural health monitoring technique that is highly sensitive to material damage initiation and propagation [1; 2]. Acoustic emission (AE) is a structural health monitoring method that is extremely sensitive to the incidence and spread of material deterioration [3; 4]. The application of AE in monitoring damage to composites has been examined by many investigations [5; 6]. Barile et al. [5] utilized AE to identify the type of damage in the carbon fiber-reinforced polymer (CFRP) samples. Wavelet packet transform (WPT) was used to decompose the AE signal. The results indicated that the signals can be classified into different categories depending on the type of damage mechanism. Xu et al. [6] applied AE to unidirectional (UD) CFRP tendons. The signals collected during the experiments were successfully used to identify damage patterns and damage evolution in unidirectional (UD) CFRP tendons during tensioning using Hilbert marginal energy spectrum (HMES) and instantaneous energy spectrum (IES).

AE has also been investigated to assess the LVI on fiber composites [7; 8]. Mal et al [7] applied AE to graphite-epoxy composite plates to detect LVI. The results showed that impact loads can be identified from the AE signals and the delamination damage can also be assessed by examining the waveform of the recorded AE signal. James et al. [8] placed four AE sensors on the CFRP specimens. Impact experiments were conducted on the specimens. The AE waveforms and

frequency spectrums obtained from the experiments were analyzed to distinguish between the different AE signatures. The analysis of the recorded AE signals made it possible to determine whether the structure has been damaged because of the impact events.

According to the investigations mentioned above, AE monitoring of the impact on fiber composite materials is promising. However, traditional analyzing methods of AE signals are usually analyzed manually based on experience and are particularly challenging, especially for complex data sets. In addition, due to environmental restrictions during aircraft operation, only a minimal number of AE sensors (i.e., a single AE sensor) could be attached to the aircraft. This further increases the difficulty of data analysis. Therefore, an intelligent approach is needed to assist in analyzing AE data in real time and alert the impact energy level. Machine learning and deep learning have been used by many studies to analyze the AE signals of composite materials. Ai et al. [9] designed a system to localize the impacts on an aircraft elevator using a single AE sensor. The authors divide the elevator (with twenty composite panels) into three zones. a random forest model and a stacked autoencoder network were employed to localize impacts to the zones where impacts occurred. The results showed that impact localization could achieve respectable results. Sikdar et al. [10] collected the AE signals on a composite panel. The AE waveforms were converted into wavelet images and served as the input of a convolutional neural network (CNN) model. Results showed an excellent zonal locational accuracy can be obtained.

This paper explored the feasibility of using a single AE sensor to identify the LVI energy levels on an aircraft elevator. The AE signals caused by the impacts with five different impact energies were recorded. A method was proposed to evaluate the impact energy and classify the impacts into various energy levels by leveraging continuous wavelets transform (CWT) and convolutional neural network (CNN).

2. METHODOLOGY

LVI energy assessment

AE is a physical phenomenon caused by the quick release of elastic energy when fractures or defects emerge in materials. AE signals can be detected and collected by placing AE sensors on the surface of an object. AE monitoring is the process of recording and processing AE signals to examine the health condition of the object. An impact energy assessment method for aircraft elevators was suggested in this paper.

During the flight, AE signals caused by LVI may be recorded by a single AE sensor and saved as time series waveforms. CWT is utilized to extract time-frequency features and convert the time series AE waveforms into RGB images. A deep residual convolutional neural network model is employed to identify the energy level of the impacts and

classify the impacts into five energy levels. The different procedures of the proposed method are presented in Figure 1.

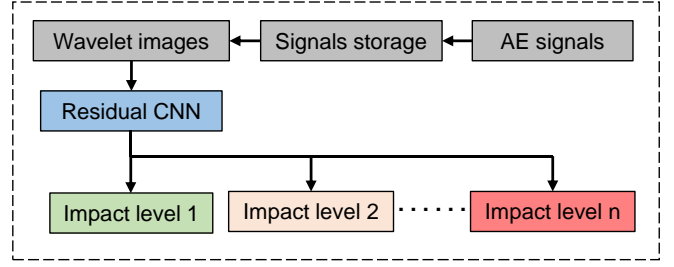


Figure 1. Workflow of the proposed method

Continuous wavelets transform

Continuous wavelets transform (CWT) captures the time-frequency properties of non-stationary signals, such as AE signals [11; 12]. The Morse wavelet is used as the mother wavelet function in this paper to conduct CWT. Eq (1) shows the Fourier transform of a Morse wavelet

$$\Psi_{p,\gamma}(x) = U(x)\alpha_{p,\gamma}x^{\frac{p^2}{\gamma}}e^{-x^\gamma} \quad (1)$$

where $U(x)$ denotes the unit step, $\alpha_{p,\gamma}$ denotes the normalizing constant, and p^2 is the time-bandwidth product, γ is the parameter that describes the Morse wavelet's symmetry [11]. p^2 and γ were defined as 60 and 3 in this paper.

The continuous wavelet coefficients can be expressed using a scalogram image. CNN models use the 2D scalogram pictures as input. The wavelet coefficients are scaled from 0 to 1 in this work.

Convolutional neural network

A convolutional neural network (CNN) is a deep neural network containing convolutional filters [13]. The input layer, the feature extraction layers, and the fully connected layer are the three primary parts of a CNN model. The essential part of the feature extraction layers includes convolutional layers and pooling layers. This paper utilized a CNN model with VGG-19 structure. VGG is developed based on the AlexNet model [14], which is a commonly used CNN structure. The number of layers was extended up to nineteen. The advantage of VGG-19 compared to AlexNet lies in replacing larger convolution kernels in AlexNet (11×11 , 7×7 , and 5×5 convolution kernels) by stacking 3×3 convolution kernels [15]. Using the stacked small convolution kernels, the number of layers and the nonlinearity of the network increases, which gives the network the ability to learn more complex features.

In this paper, the last FC layer of VGG-19 is modified to have the class number to be consistent with the number of impact energy levels. Figure 2 shows the main structure of the modified VGG-19.

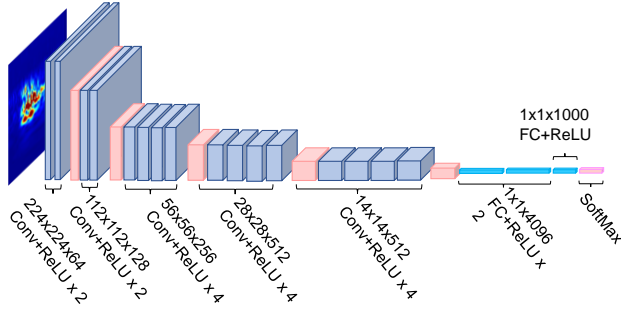


Figure 2. Modified VGG-19

3. EXPERIMENTAL DESCRIPTION

Experimental setup

In this paper, an impact experiment was conducted on a thermoplastic elevator specimen. This specimen is comprised of twenty panels that reside between 20 ribbed sections. An illustration of the elevator specimen can be seen in Figure 3. For the impact process, five steel spheres were used to create five levels of impact (level 1 to level 5). With each sphere having varying diameters of 0.006, 0.013, 0.019, 0.025, and 0.032 meters, respectively. The steel spheres are shown in Figure 4. These spheres are used to impact the elevator in a controlled and repeatable procedure. A consistent drop height of 0.61 meters was selected as the height necessary for these impacts.

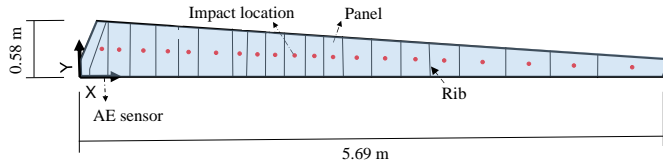


Figure 3. Elevator specimen



Figure 4. Steel spheres

In order to maintain proper drop height and drop location during the experiment, a guide tube was used. This can be seen in Figure 5. The five spheres have impact energies of 0.006 J, 0.05 J, 0.17 J, 0.38J, and 0.75 J reactively, the impact energies will be defined as energy levels 1 to 5. Each panel of the elevator was impacted by each sphere 60 times each. The impact sites are presented as red points in Figure 3. As the elevator was impacted, an AE sensor attached to the front spar of the elevator can monitor the impacts and record the AE signals. Each energy level produces 1200 AE signals, meaning a total of 6,000 AE signals were captured.

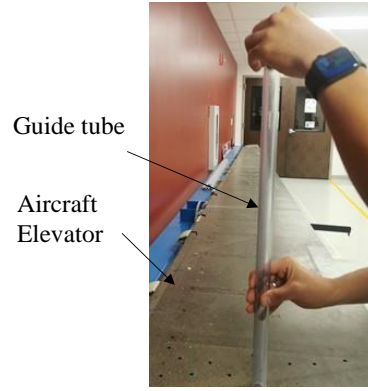


Figure 5. Steel sphere impact

Acoustic Emission Instrumentation and Setup

A PAC micro-30 was used for the AE sensor. It has an operating frequency range of 150 - 400 kHz. AE signals were acquired by a 16-channel system. A pre-trigger time of 256 μ s was used, this is done to recover AE waveforms before the threshold crossing. The sampling rate was 1 MHz. The signal length was 2,048 microseconds. The peak definition time (PDT) was set as 200 μ s, this refers to the time between the first threshold crossing to the peak amplitude, and the hit definition time (HDT) was set to 400 μ s. The hit lockout time (HLT) was set to 400 μ s, this prevents recording late-arriving signals and reflected hits.

4. RESULTS AND DISCUSSION

Input preparation

During the impact experiment, the dropping of the steel spheres on each elevator panel was repeated 60 times. In total, 6,000 impact events were detected and recorded by the AE acquisition system. Each of the AE signals is a time series with 2,048 sample points since the acquisition sampling rate was set to 1 MHz and the duration was 2,048 microseconds. All amplitudes of AE signals were normalized to -1 to 1. The waveforms of the normalized signals that were arbitrarily chosen from each energy level are displayed in Figure 4. The AE waveforms were used to construct CWT coefficients. The time-frequency component within the signal was then better displayed by converting the Y-axis of the CWT coefficient to a logarithmic coordinate. The coefficients were saved as RGB images with a size of 224 by 224 by 3 (Figure 6).

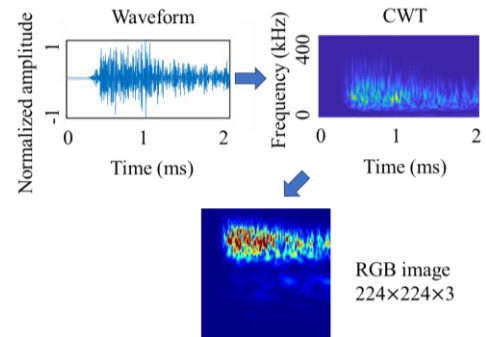


Figure 6. AE waveform and CWT coefficient

Energy assessment

The LVI energy level is determined by assigning the AE signals to a CNN model after they have been transformed into RGB pictures. In the 6,000 data events collected during the experiment, 4,200 AE data were randomly selected for training, and 600 AE data were randomly selected for validation. The remaining 1,200 data were utilized to test the performance of the trained CNN. The optimizing approach of the CNN model in the impact energy identification module was the Adaptive moment estimation method (Adam). The batch size was 32, the learning rate was 0.0001. The training, validating, and testing processes were executed on a workstation with a CPU-R9 5900HX, 4.6GHz, 32GB RAM, and a GPU-RTX3080, 16 GB GDDR6. The energy assessment results are shown in Figure 7 as a confusion matrix. The numbers of AE data that are correctly classified in their corresponding energy levels are shown in the main diagonal of the confusion matrix. There were 1,108 AE events correctly classified, accounting for 94.3% of the total AE data. In other words, the overall accuracy was 94.3%. To be more specific, the number of the AE data that were correctly classified to the correct energy level zones is respectively 231 in level 1, 228 in level 2, 218 in level 3, 231 in level 4, and 224 in level 5.

		Recall				
Actual energy level	1	231	6	2	1	96.3%
	2	5	228	3	4	95.0%
	3		7	218	9	90.8%
	4			7	231	96.3%
	5			12	4	93.3%
Precision		97.8%	94.6%	90.1%	92.8%	96.6%
		1	2	3	4	5
		Evaluated energy level				

Figure 7. Confusion matrix of impact energy assessment

In addition to accuracy, precision and recall for each class are usually implemented to evaluate the performance of classification in each class [16]. The value of precision is obtained by Eq. (2):

$$Precision = \frac{TP}{TP+FP} \quad (2)$$

Where TP refers to true positives, which means the number of samples that correctly classify to the corresponding class, FP refers to false positives, which is the number of samples that do not belong to the class but are classified into the class by error. Precisions of the five class are respectively 97.8%, 94.6%, 90.1%, 92.8%, 96.6% from energy levels 1 to 5.

Eq. (3) can obtain the value of recall:

$$Recall = \frac{TP}{TP+FN} \quad (3)$$

Where FN refers to false negatives, the number of samples that belong to the class but are classified into the other classes by error. Recalls of the five classes are respectively 96.3%, 95.0%, 90.8%, 96.3%, 93.3% from zone 1 to 5.

Precision and recall influence each other. A class with high precision usually has a low recall and vice versa [16]. To comprehensively evaluate the efficiency of the classifier in each class, the F1-score can be employed. F1-score, also referred to as the balanced F score, is defined as the harmonic mean of precision and recall [17]. F1 score can be calculated by Eq. (4):

$$F1 = \frac{2 \times Precision \times Recall}{Precision + Recall} = \frac{2TP}{2TP + FP + FN} \quad (4)$$

F1 of the five classes are respectively 97.0%, 94.8%, 90.4%, 94.5%, 94.9% from energy levels 1 to 5.

The recall, precision, and F1 of the five classes are higher than 90%. Therefore, it can be concluded that the impact energy identification module proposed in this paper has acceptable performance at different energy levels.

Cross-validation

AE signals were divided into five equal-sized, mutually exclusive groups (A, B, C, D, and E). Through these groups, five-fold cross-validation was conducted. The reliability of the proposed method can be evaluated effectively while avoiding overfitting and underfitting [18; 19]. Results are presented in Table 1. All five iterations yield steady results that are close to the average value. This finding shows that the LVI energy assessment approach is dependable. The divide between the training and testing set has a minor effect on performance.

Table 1. Results of five-fold cross-validation

Train/Testing	Accuracy
(A, B, C, D), E	94.3%
(A, B, C, E), D	94.6%
(A, B, D, E), C	93.9%
(A, C, D, E), B	93.7%
(B, C, D, E), A	94.2%
Average	94.1%

5. CONCLUSIONS

This paper focuses on the LVI detection of an aircraft elevator using one AE sensor. An AE method was proposed to assess the energy level of the impacts. A deep residual CNN model with the structure of VGG-19 was utilized for the impact energy assessment. To validate the performance of the proposed method, an impact experiment was designed. The AE signals of five impact energies (impact levels 1 to 5) were collected on an aircraft elevator specimen using steel spheres with five different diameters. Acceptable accuracy (94.3%) for LVI energy assessment can be observed. The cross-validation also indicates the reliability of the method.

These findings show that the method proposed in this paper has respectable performance.

This method can potentially be utilized for LVI monitoring of aircraft control panels and also for the impact monitoring of urban air mobility. The limitation of this study is that only five energy levels of LVI were considered, future studies should include more energy levels or develop a regression model that can predicts energy.

ACKNOWLEDGMENT

This paper was partially supported through the National Aeronautics and Space Administration (NASA) under the University Leadership Initiative program; grant number 80NSSC20M0165. The views and opinions of the authors expressed herein do not necessarily state or reflect the opinions of the funding agency or agencies.

REFERENCES

- [1] L. Ai, V. Soltangharai, M. Bayat, B. Greer, P. Ziehl, 2021. Source localization on large-scale canisters for used nuclear fuel storage using optimal number of acoustic emission sensors, *Nuclear Engineering and Design* 375 111097.
- [2] V. Soltangharai, R. Anay, L. Ai, E.R. Giannini, J. Zhu, P. Ziehl, 2020. Temporal evaluation of ASR cracking in concrete specimens using acoustic emission, *Journal of Materials in Civil Engineering* 32 04020285.
- [3] L. Ai, V. Soltangharai, P. Ziehl, 2022. Developing a heterogeneous ensemble learning framework to evaluate Alkali-silica reaction damage in concrete using acoustic emission signals, *Mechanical Systems and Signal Processing* 172 108981.
- [4] R. Anay, A. Lane, D.V. Jáuregui, B.D. Weldon, V. Soltangharai, P. Ziehl, 2020. On-Site Acoustic-Emission Monitoring for a Prestressed Concrete BT-54 AASHTO Girder Bridge, *Journal of Performance of Constructed Facilities* 34 04020034.
- [5] C. Barile, C. Casavola, G. Pappaletta, P.K. Vimalathithan, 2019. Damage characterization in composite materials using acoustic emission signal-based and parameter-based data, *Composites Part B: Engineering* 178 107469.
- [6] J. Xu, W. Wang, Q. Han, X. Liu, 2020. Damage pattern recognition and damage evolution analysis of unidirectional CFRP tendons under tensile loading using acoustic emission technology, *Composite Structures* 238 111948.
- [7] A.K. Mal, F. Shih, S. Banerjee, 2003, Acoustic emission waveforms in composite laminates under low velocity impact, *SPIE*, 1-12.
- [8] R. James, R.P. Joseph, V. Giurgiutiu, 2021. Impact damage ascertainment in composite plates using in-situ acoustic emission signal signature identification, *Journal of Composites Science* 5 79.
- [9] L. Ai, V. Soltangharai, M. Bayat, M. van Tooren, P. Ziehl, 2021. Detection of impact on aircraft composite structure using machine learning techniques, *Measurement Science and Technology* 32 084013.
- [10] S. Sikdar, D. Liu, A. Kundu, 2022. Acoustic emission data based deep learning approach for classification and

detection of damage-sources in a composite panel, Composites Part B: Engineering 228 109450.

- [11] L. Ai, V. Soltangharai, P. Ziehl, 2021. Evaluation of ASR in concrete using acoustic emission and deep learning, Nuclear Engineering and Design 380 111328.
- [12] W. Zhou, Z. Feng, Y. Xu, X. Wang, H. Lv, 2022. Empirical Fourier decomposition: An accurate signal decomposition method for nonlinear and non-stationary time series analysis, Mechanical Systems and Signal Processing 163 108155.
- [13] A. Krizhevsky, I. Sutskever, G.E. Hinton, 2012, Imagenet classification with deep convolutional neural networks, 1097-1105.
- [14] K. Simonyan, A. Zisserman, 2014. Very deep convolutional networks for large-scale image recognition, arXiv preprint arXiv:1409.1556.
- [15] A. Krizhevsky, I. Sutskever, G.E. Hinton, Imagenet classification with deep convolutional neural networks, 2012, 1097-1105.
- [16] M. Buckland, F. Gey, 1994. The relationship between recall and precision, Journal of the American society for information science 45 12-19.
- [17] R. Yacouby, D. Axman, 2020, Probabilistic extension of precision, recall, and F1 score for more thorough evaluation of classification models, 79-91.
- [18] C. Lim, B. Yu, 2016. Estimation stability with cross-validation (ESCV), Journal of Computational and Graphical Statistics 25 464-492.
- [19] S. Bates, T. Hastie, R. Tibshirani, 2021. Cross-validation: what does it estimate and how well does it do it?, arXiv preprint arXiv:2104.00673.



Bryson Henderson is a research assistant at the University of South Carolina. His current research topic is numerical modeling for aerospace structures. He is currently working towards his bachelor's degree in Aerospace Engineering



Sydney Houck is a research assistant at the University of South Carolina. Her current research topic is minimally intrusive sensing for urban air mobility. She is currently pursuing her bachelor's degree in Mechanical Engineering

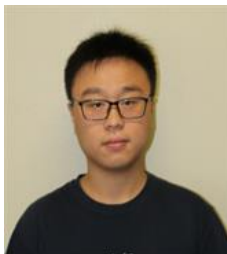


Samuel Dickson is a research assistant at the University of South Carolina. He has worked on several projects involving damage sensing and material science. He is now pursuing a bachelor's degree in Aerospace Engineering.



Paul Ziehl received a Ph.D. in Civil Engineering from the University of Texas at Austin in 2000. Currently he serves as the Associate Dean for Research and Professor in the College of Engineering and Computing at the University of South Carolina. His research interests include adaptive structures, remote monitoring, and predictive analytics

BIOGRAPHY



Li Ai received a Ph.D. in Civil Engineering from the University of South Carolina in 2021. He is currently a postdoctoral fellow in the same university. His current research interests include numerical modeling, machine learning and their applications in structural health monitoring.